JMEPEG (2010) 19:1330–1336
DOI: 10.1007/s11665-010-9607-3

1059-9495/$19.00

Effect of Al_2O_3 Content on Electrical Breakdown Properties of Al_2O_3/Cu Composite

Xianhui Wang, Shuhua Liang, Ping Yang, and Zikang Fan

(Submitted March 31, 2009; in revised form January 19, 2010)

Al_2O_3/Cu composites were prepared by external addition of Al_2O_3, and the effect of Al_2O_3 content on microstructure, density, hardness, electrical conductivity and vacuum electrical breakdown properties was studied. The results show that with increasing Al_2O_3 addition, the density of Al_2O_3/Cu composite significantly decreases, the hardness sharply increases and then slowly decreases, but the electrical conductivity invariably decreases. The vacuum breakdown test shows that with increasing Al_2O_3 addition, the breakdown strength first sharply increases and then decreases when the Al_2O_3 content exceeds 1.2 wt.%; the chopping current always exhibits a decreasing trend and the arc life first increases and then decreases. According to the morphology of arc erosion and analysis, the arc erosion resistance increases and then decreases sharply. In the range of experiments, the optimal arc erosion resistance of Al_2O_3/Cu composite can be obtained with the addition of 1.2 wt.% Al_2O_3.

Keywords Al_2O_3/Cu composite, electron microscopy, powder metallurgy

1. Introduction

Due to its high strength and good conductivity at elevated temperatures, the Al_2O_3/Cu composite, which is regarded as an ideal substitute for high conductive copper alloy, has wide potential applications in the electrical contact and electrode materials, lead frame, express train overhead conductors and connector (Ref 1-4). Most studies focus on the microstructure, physical and electrical properties of Al_2O_3/Cu composite (Ref 5-14), but no literatures on the relationship between microstructure and arc erosion behavior of Al_2O_3/Cu composite have been reported. In this investigation, Al_2O_3/Cu composite was prepared by external addition of Al_2O_3 and the effect of Al_2O_3 content on hardness, electrical conductivity, breakdown strength, chopping current and arc life was studied. The relationship of microstructure and arc erosion behavior was disclosed and it is hoped that this research can provide the reference for the design of oxide/metal system contact materials and the arc control.

2. Experimental

Cu powders with a purity of 99 wt.% and the particle size of 50 μm and 0.4 wt.%, 0.8 wt.%, 1.2 wt.%, 1.6 wt.% and 2.0 wt.% Al_2O_3 powders with a purity of 99.5 wt.% and the average size of 30 nm were milled for 12 h respectively under argon gas at a ball-to-powder mass ratio of 10:1 and a rotation rate of 200 rpm. The milled powders were hot-pressed and sintered at 950 °C in a XP-80B sintering furnace. For convenience, those samples with different contents of Al_2O_3 particles prepared were designated as samples No. 1-No. 5. The density was measured by utilizing Archimedes' method and the electrical conductivity and hardness tests were performed on a 7501 eddy-current instrument and a HB-3000 Brinell hardness tester, respectively, and the mean values were the average of three measured results. The vacuum breakdown was tested on a modified TDR240A single crystal furnace, in which the power circuit was illustrated schematically in Fig. 1. After polishing, the samples were put in a sample holder as a cathode, which could move vertically in the vacuum chamber. Above the cathode there was a pure tungsten rod with a radius of 5 mm and a tip radius of about 1 mm as an anode. When the chamber was evacuated to 5.0×10^{-3} Pa and the capacitor of 120 μF was charged to the voltage (V) of 9 kV, the lower cathode moved upward at a velocity of 0.2 mm/min until the gap was broken down. Meanwhile, the discharged waveform and the parameters were recorded by a Tektronix TDS-2014 dual channel digital memory oscilloscope (200 MHz) and the gap (D) between the cathode and the anode (breakdown distance) was measured. The breakdown voltage was calculated by V/D. The mean values of breakdown voltage and chopping current were calculated by the average of 100 measured values. The microstructures of the Al_2O_3/Cu composites after electrical breakdown were characterized by an OXFORD JSM-6700F field emission scanning electron microscope (SEM). The spatial distribution of Al_2O_3 particles in Cu matrix was evaluated by the enumeration method proposed by Xie et al. (Ref 15), which can be described as follows. First a given area, in which the number of reinforcement particles is above 300, is photographed and copied. The area is then divided into N micro-areas, in which the number of reinforcement particles is at least 20. The number of particles in each micro-area (Z_i) and the average number of particles in unit micro-area ($\bar{Z}$)

Xianhui Wang, Shuhua Liang, Ping Yang, and **Zikang Fan**, School of Materials Science and Engineering, Xi'an University of Technology, Xi'an 710048, P.R. China. Contact e-mail: liangsh@xaut.edu.cn.

can be determined. Hence, the relative standard deviation of particles in the micro-area (S'_{rel}) can be written as:

$$S'_{rel} = \frac{\sqrt{\frac{1}{(N-1)}\sum_{i=1}^{N}(Z_i - \bar{Z})^2}}{\bar{Z}} \times 100\% \quad \text{(Eq 1)}$$

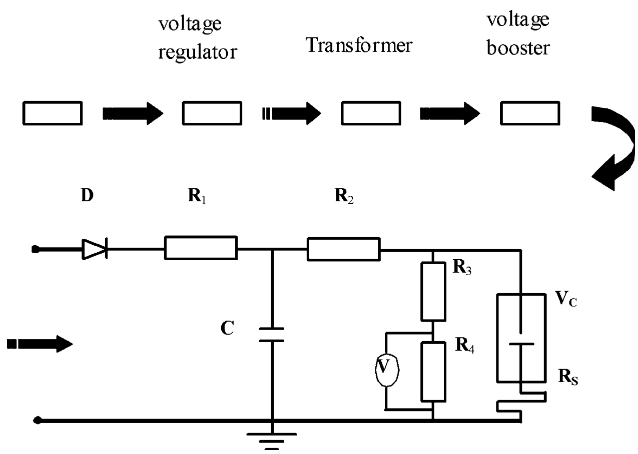

Fig. 1 The circuit of high-voltage vacuum electrical breakdown

where N is the total number of micro-areas, $\bar{Z}$ is the average number of particles in a micro-area, and Z_i is the number of reinforcement particles in each micro-area.

The numbers of reinforcement particles were counted utilizing Image-pro plus 6.0 software, and the calculated S'_{rel} was used to characterize the distribution of reinforcement particles in different micro-areas. The less S'_{rel} represents a more uniform distribution of the reinforcement particles. As the spacing between particles was not considered in the method, the agglomeration of reinforcement particles could not be estimated. Subsequently, the spatial distribution and agglomeration were evaluated by micrographs along with the enumeration method.

3. Results and Discussion

3.1 Microstructure of Al_2O_3/Cu Composites

The microstructures of Al_2O_3/Cu composites with different contents of Al_2O_3 are shown in Fig. 2(a)-(e), respectively. It can be seen from Fig. 2 that the distribution of Al_2O_3 particles is relatively uniform on the Cu matrix at the low contents of Al_2O_3, see Fig. 2(a) and (b). When the Al_2O_3

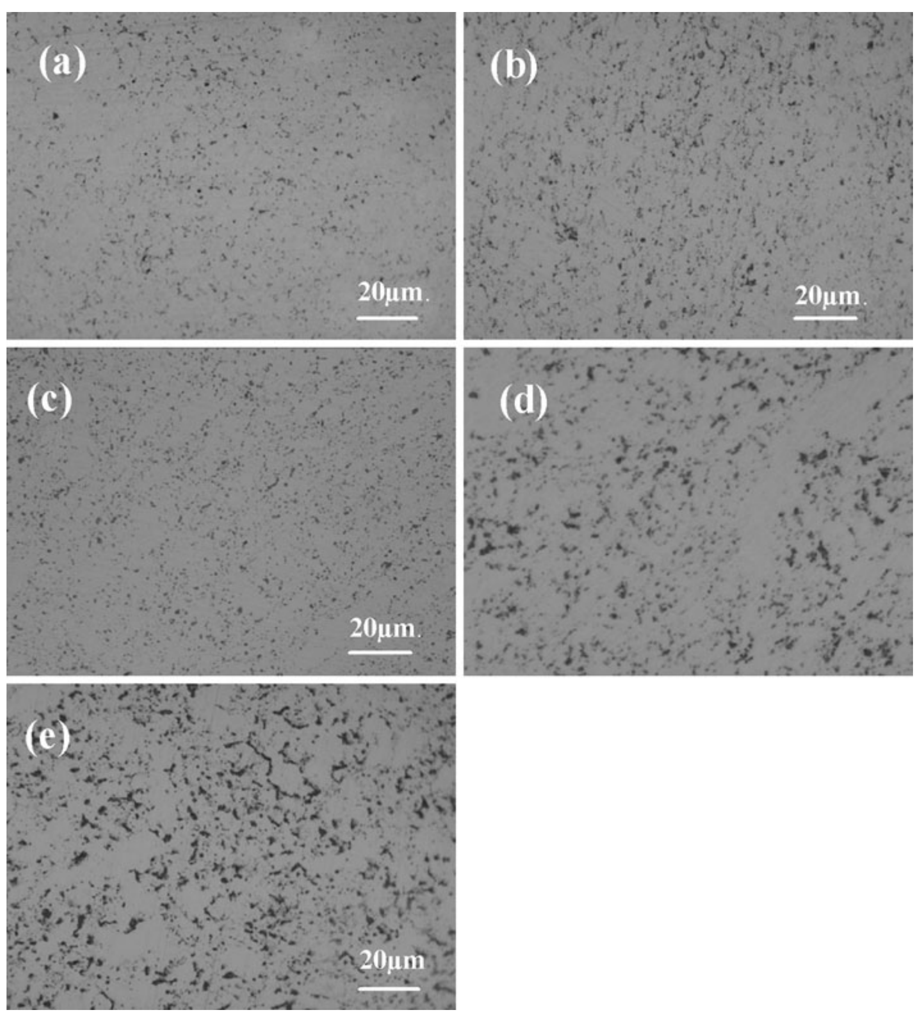

Fig. 2 Microstructures of Al_2O_3/Cu composites with different contents of Al_2O_3: (a) 0.4 wt.%, (b) 0.8 wt.%, (c) 1.2 wt.%, (d) 1.6 wt.% and (e) 2.0 wt.%

content is above 1.2 wt.%, Al_2O_3 particles are agglomerated and the spacing between particles gradually decreases (Fig. 2c). However, when the Al_2O_3 content exceeds 1.6 wt.%, there exists an obvious agglomeration, as shown in Fig. 2(d) and (e).

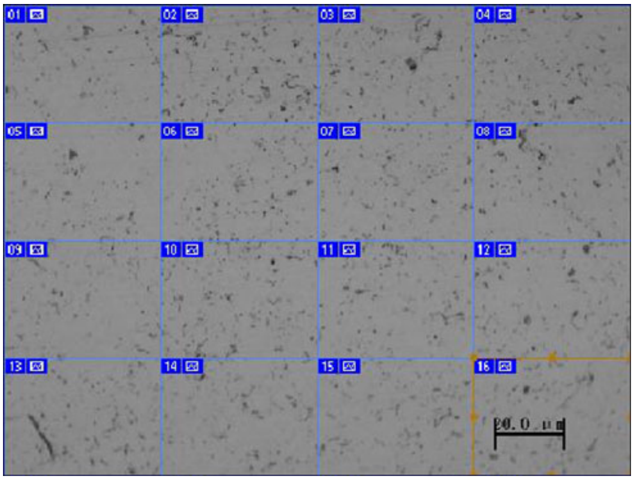

Fig. 3 The subdivision photograph of sample No. 1

3.2 Quantitative Analysis of the Uniformity of Al_2O_3 Distribution

In order to quantitatively evaluate the distribution of Al_2O_3 particles, sample No. 1 is taken as an illustrative example. First, Fig. 2(a) was subdivided into 16 areas using Photoshop software, labeled as 01, 02, 03, 04,…, 16 in Fig. 3. Secondly, the numbers of Al_2O_3 particles in different micro-areas illustrated in Fig. 4(a)-(d) were counted by Image-pro plus 6.0 software. The statistical data in each micro-area are listed in Table 1. According to Eq 1, then $S'_{rel} = 0.1547$.

Similarly, other S'_{rel} can also be calculated by utilizing the same method and the results are given in Table 2.

From Table 2, it can be seen that with increase of Al_2O_3 content, the relative standard deviation gradually decreases in the range of 0.4-1.2 wt.% Al_2O_3. It indicates that the spatial distribution of Al_2O_3 particles becomes uniform. However, if the Al_2O_3 content exceeds 1.2 wt.%, the relative standard deviation increases, suggesting the worse spatial distribution of Al_2O_3 particles at higher Al_2O_3 content.

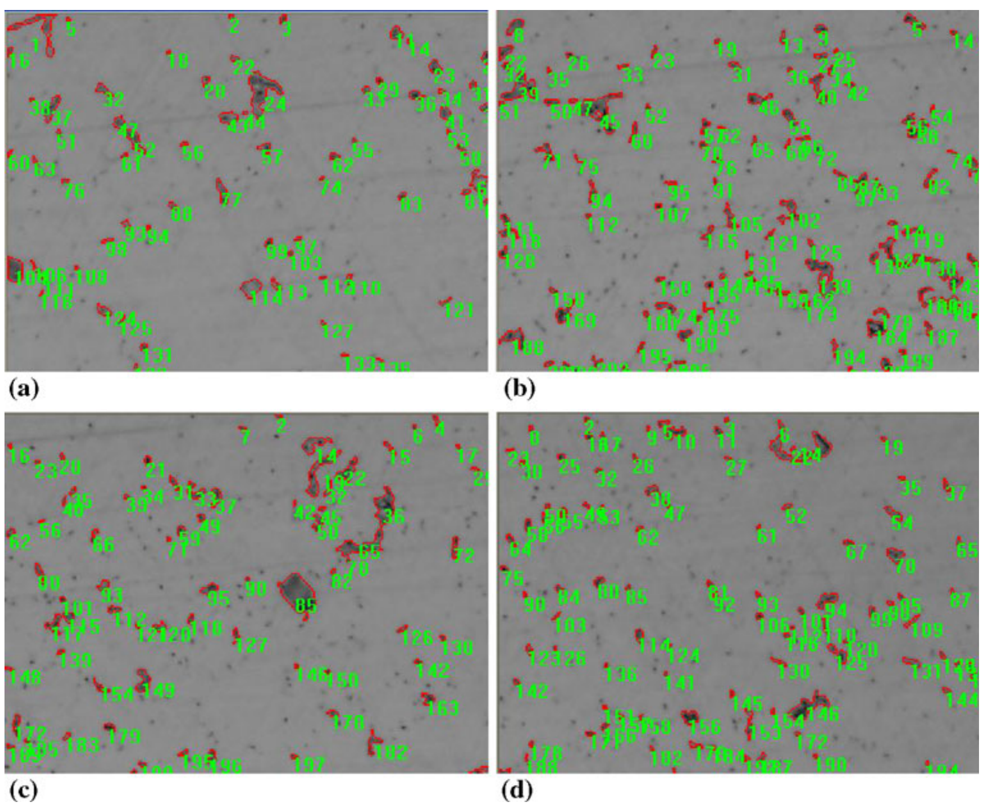

Fig. 4 The counting number of Al_2O_3 particles in four different microareas

Table 1 The number of Al_2O_3 particles in each microarea of sample No. 1

	Subdivision image no.															
	1	2	3	4	5	6	7	8	9	10	11	12	13	14	15	16
Number of Al_2O_3 particles	141	212	206	202	144	210	218	148	175	210	186	178	155	162	149	204

Table 2 Variation of the relative standard deviation of particles with Al_2O_3 content

	Sample no.				
	1	2	3	4	5
Al_2O_3 content, wt.%	0.4	0.8	1.2	1.6	2.0
Relative standard deviation	0.1547	0.1513	0.1079	0.2692	0.3174

Table 3 Physical properties of Al_2O_3/Cu composites

Sample no.	Al_2O_3 volume fraction, vol.%	Relative density, %	Hardness, HB	Electrical conductivity, IACS%	Thermal conductivity, W/k m
1	3.48	99.41	75	94.1	370.57
2	6.81	98.73	90	93.3	349.39
3	8.81	97.52	125	86.2	337.21
4	12.59	93.66	123	80.0	315.23
5	14.95	87.35	119	74.0	302.14

3.3 Physical Properties of Al_2O_3/Cu Composites

Table 3 presents the results of relative density, hardness and electrical conductivity of Al_2O_3/Cu composites. From Table 3, the densification and electrical conductivity of Al_2O_3/Cu composite significantly decrease with increasing the Al_2O_3 content. In comparison with values reported in the literatures (Ref 12-14), the electrical conductivity is higher for Al_2O_3/Cu composite prepared at this research activity. The hardness increases sharply and then decreases slightly. At 1.2 wt.% Al_2O_3, Al_2O_3/Cu composite has the maximum hardness value of 125HB.

The thermal conductivity of a composite can be predicted by Eq 2 (Ref 16):

$$K_c = K_m \cdot \frac{1 + 2V_r \cdot \frac{1-K}{1+2K}}{1 - V_r \cdot \frac{1-K}{1+K}} \quad \left(K = \frac{K_m}{K_r}\right) \qquad \text{(Eq 2)}$$

where K_c, K_m and K_r are the thermal conductivity of the composite, the matrix, the reinforcement phase, respectively, and V_r is the volume fraction of the reinforcement phase in the composite. For Cu matrix and Al_2O_3 reinforcement phase, K_m = 394 W/m/K, K_r = 30 W/m/K.

According to Eq 2, the thermal conductivity can be calculated and the results are also given in Table 3. As seen in Table 3, the thermal conductivity of Al_2O_3/Cu composites decreases with increase of Al_2O_3 content. Sample No. 1 with 3.48 vol.% Al_2O_3 shows a thermal conductivity of 370.57 W/m/K. However, the thermal conductivity of the Al_2O_3/Cu composite with 14.95 vol.% Al_2O_3 decreases dramatically. This can be understood by the variation of the relative density of the composites with different volume fraction of Al_2O_3 after sintering. In comparison with sample No. 1 with 3.48 vol.% Al_2O_3, the relative density of sample No. 5 with 14.95 vol.% Al_2O_3 is much lower, which is decreased by approximately 12.13%. Subsequently, the poor densification results in the remarkable decrease in the thermal conductivity.

Table 4 Electrical breakdown results of Al_2O_3/Cu composites with different contents of Al_2O_3

	Sample no.				
	1	2	3	4	5
Al_2O_3 content, wt.%	0.4	0.8	1.2	1.6	2
Breakdown strength, $\times 10^7$ v/m	4.616	5.249	5.669	5.422	5.081
Chopping current, A	4.63	3.75	3.51	3.53	3.48
Arc life, ms	15.55	17.47	17.94	17.28	16.35

3.4 The Effect of Al_2O_3 Content on the Breakdown Strength, Chopping Current and Arc Life of Al_2O_3/Cu Composites

The electrical breakdown results of Al_2O_3/Cu composites with different contents of Al_2O_3 are presented in Table 4. It can be seen that the breakdown strength dramatically increases and then decreases with increasing Al_2O_3 content. The Al_2O_3/Cu composite has the maximum breakdown strength of 5.669×10^7 v/m at 1.2 wt.% Al_2O_3. The arc life has a similar trend as the breakdown strength. However, the chopping current invariably decreases.

The variation of breakdown strength is caused by the interaction of hardness, viscosity and densification. With increasing Al_2O_3 content, the spacing between Al_2O_3 particles decreases, and, thus, increases the strengthening effect and hardness of Al_2O_3/Cu composites. Meanwhile, the viscosity of molten layer during breakdown increases with increasing Al_2O_3 content. When the Al_2O_3/Cu composite is subjected to breakdown many times, its surface is melted and cooled repeatedly, thus smoothing the surface and enhancing the breakdown voltage. However, when the Al_2O_3 content is above 1.2 wt.%, the breakdown strength is significantly decreased due to the low densification, Al_2O_3 serious agglomeration, and high gas content in the Al_2O_3/Cu composite.

It is also learnt from Table 3 that the thermal conductivity of Al_2O_3/Cu composites decreases with increasing Al_2O_3 particles. At the low thermal conductivity, the thermal energy in the breakdown microarea, which cannot be transferred in time, can be easily accumulated, thus resulting in a severe vaporization in this area and a longer arcing time. Subsequently, the electrical current is much easily chopped at a lower level. Since alumina has a low work function and the increased Al_2O_3 lowers the consumed energy by the electron emission of cathode, the same input energy into the cathode causes a higher temperature on the surface of cathode, thus making the material vaporize easily, improving the metallic vaporization pressure and lowering the chopping current. In addition, the enhanced electron scattering, due to the increased Al_2O_3 content, results in the increase in the electrical resistivity, decrease in the chopping current and the prolong arc life as well.

3.5 The Effect of Al_2O_3 Content on the Arc Erosion of Al_2O_3/Cu Composites

Figure 5 shows the surface morphologies of Al_2O_3/Cu composites with different contents of Al_2O_3 after breakdown 100 times. Figure 5(a)-(d) are the entire erosion images of Al_2O_3/Cu composites with 0.4 wt.%, 1.2 wt.%, 1.6 wt.% and 2.0 wt.% Al_2O_3, respectively, while Fig. 5(a1)-(d1) are the central erosion morphologies of the corresponding samples.

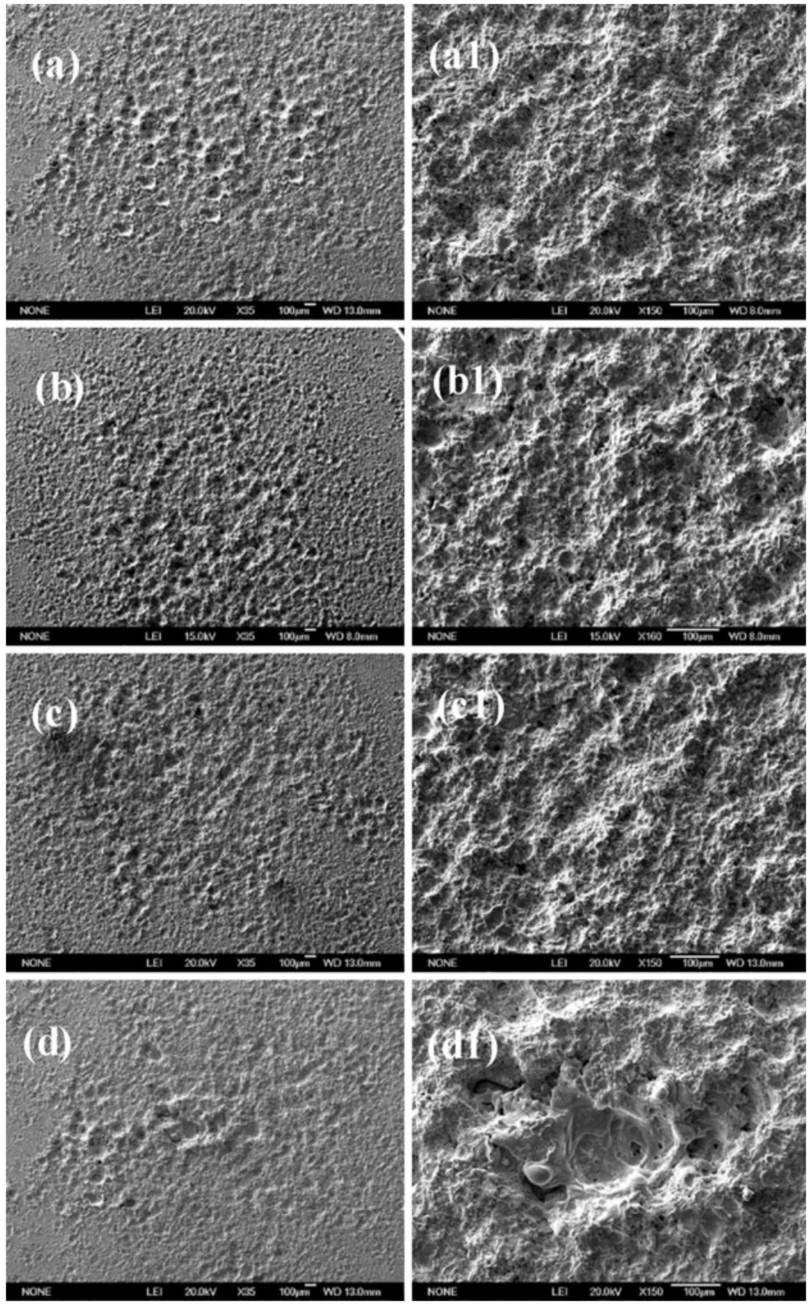

Fig. 5 SEM micrographs of Al_2O_3/Cu composites after vacuum breakdown 100 times: (a) 0.4 wt.%, (b) 1.2 wt.%, (c) 1.6 wt.%, and (d) 2.0 wt.%. The images (a1)-(d1) are the magnifying images of (a)-(d), respectively

It can be seen from Fig. 5 that the erosion area increases and then decreases with the increased Al_2O_3 content. When the Al_2O_3 content is 0.4 wt.%, there are characteristics of relatively concentrated arc erosion, deep erosion pits formed by sputtering, and distinct boundaries among erosion pits. It suggests that the arc motion presents in a hopping way as shown in Fig. 5(a) and (a1). From Fig. 5(b)-(b1) and (c)-(c1), the amount of erosion pits and erosion area are increased, some small erosion pits present at the edge of samples 3 and 4 and the boundaries among erosion pits in the central region fold with each other. It indicates that arc spread out in the surrounding area. When the Al_2O_3 content is 2.0 wt.%, arc erosion trends to be concentrated again and large erosion pits are formed as shown in Fig. 5(d) and (d1).

Nano-sized Al_2O_3 particles, due to high surface energy, are easily aggregated if Al_2O_3 content exceeds a certain value in the molten copper alloy, thus destroying the dispersive stability. Under the repeatable arcing, a large amount of nano-sized Al_2O_3 particles will be floated and agglomerated, and, if serious, cause the formation of cracks. Such erosion defects for the Al_2O_3/Cu composites with 1.6 wt.% and 2 wt.% Al_2O_3 are shown in Fig. 6(a) and (b).

From viewpoints of the preparing technology, the increase in Al_2O_3 content will cause the decreased densification of Al_2O_3/Cu composites, and the increased gas content and a large mount of porosity. When the thermal energy is sufficiently high in the erosion area, the gas trapped in the Al_2O_3/Cu composite escapes from surface, thus resulting in spattering and the

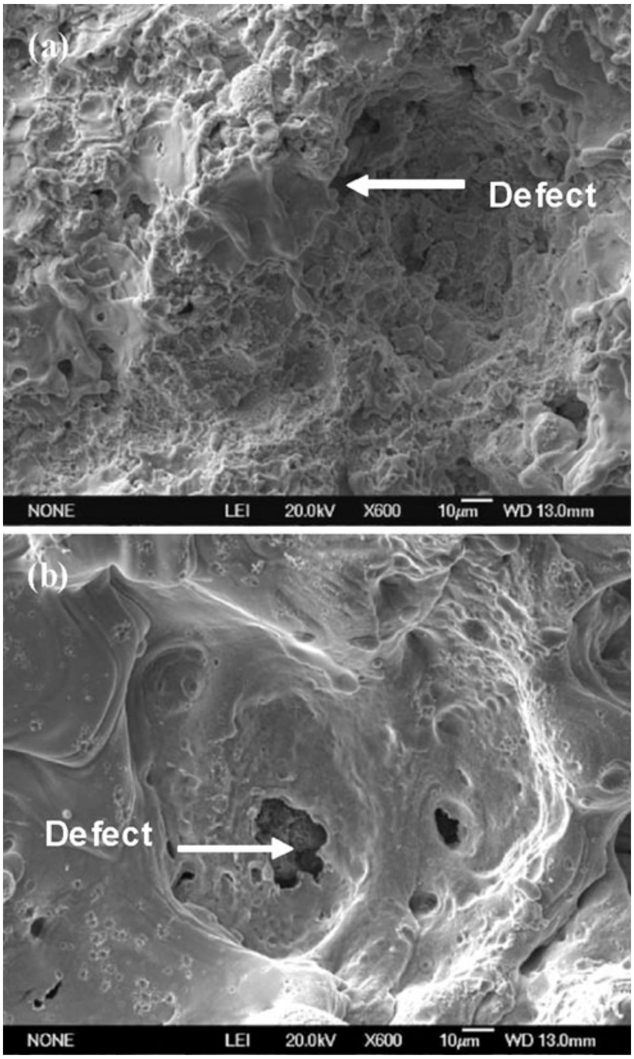

Fig. 6 Defects in arc erosion zones of Al_2O_3/Cu composites with different contents of Al_2O_3: (a) 1.6 wt.% Al_2O_3 and (b) 2.0 wt.% Al_2O_3

protrusion at the edge, as marked in Fig. 6. When the electrical current is chopped once again, it is much easier to strike arc, resulting in the decrease of breakdown strength.

According to the arc motion theory and arc partition model (Ref 17), the low concentration of Al_2O_3 particles with a low work function cause the large spacing between Al_2O_3 particles. Hence, the spacing between these preferred breakdown areas becomes larger and the repel force between arcs decreases, arc trends to propagate slowly from the center of a tiny area to the surrounding area. Subsequently, arc is generated and sustained in the copper matrix, and the arc has a poor mobility and dwells in the breakdown area until it is extinguished.

With increase of Al_2O_3 particles, the spacing between Al_2O_3 particles decreases, and the spacing between the preferred breakdown areas decreases, thus providing a more effective repel force. Arc trends to propagate rapidly from the center of a tiny area to the surrounding area and moves outside until its energy cannot sustain its combustion. At this case, the Al_2O_3/Cu composite has smooth surface and higher breakdown strength. This can be verified by the morphologies of Al_2O_3/Cu composites with 1.6 wt.% and 2.0 wt.% Al_2O_3 in the erosion regions (see Fig. 5c, d).

However, if the concentration of Al_2O_3 particles exceeds a contain value, the spacing between Al_2O_3 particles becomes too small. Then, these single tiny arcs generated at many breakdown areas gather and form a large arc, i.e. the single large arc breakdown area includes a number of tiny preferred breakdown areas. As the large arc has higher energy, the surface of Al_2O_3/Cu composite is eroded seriously. Hence, the arc dwells in this region and has a worse mobility, thus resulting in the erosion for a long time. Meanwhile, with increase of gas and porosity, it is much easier for arc to generate in porosity. Therefore, the erosion pits become more concentrated and much deeper with increase of Al_2O_3 content.

4. Conclusions

The effect of Al_2O_3 content on microstructure, density, hardness, electrical conductivity and vacuum electrical breakdown properties was studied and discussed in the present investigation, and the following conclusions can be obtained:

1. With increase of Al_2O_3 addition, the density of Al_2O_3/Cu composite decrease significantly, the hardness increases sharply and then decreases slowly, but the electrical conductivity invariably decreases.
2. With increase of Al_2O_3 addition, the breakdown strength increases dramatically, and then decreases when the Al_2O_3 content exceeds 1.2 wt.%; the chopping current always has a trend to decrease; the arc life increases and then decreases.
3. The arc erosion resistance increases and then decreases sharply with increase of Al_2O_3 addition. In the range of experimental parameters, the optimal arc erosion resistance of Al_2O_3/Cu composite can be obtained with the addition of 1.2 wt.% Al_2O_3.

Acknowledgments

This research was supported by Specialized Research Fund for the Doctoral Program of Higher Education (SRFDP20060700011), Program for New Century Excellent Talents in University (NCET-05-0873) and the National Natural Science Foundation of China (Project 50574075).

References

1. J.S. Kiang, Y. Ni, and W.T. Wu, Critical Al Content to Form External-Alumina Scales on Cu-Al Alloys, *Intermetallics*, 2007, **15**, p 635–638
2. M.X. Guo, M.P. Wang, L.F. Cao, and R.S. Lei, Work Softening Characterization of Alumina Dispersion Strengthened Copper Alloys, *Mater. Charact.*, 2007, **58**(10), p 928–935
3. T.S. Srivatsan, N. Narendra, and J.D. Troxell, Tensile Deformation and Fracture Behavior of an Oxide Dispersion Strengthened Copper Alloy, *Mater. Des.*, 2000, **21**, p 191–198
4. K.X. Song, J.D. Xing, and B.H. Tian, Influence of Annealing Treatment on the Properties and Microstructures of Alumina Dispersion Strengthened Copper Alloy, *Trans. Nonferrous Met. Soc. China*, 2005, **15**(1), p 139–143
5. B.H. Tian, P. Liu, K.X. Song, Y. Li, Y. Liu, F.Z. Ren, and J.H. Su, Microstructure and Properties at Elevated Temperature of a

Nano-Al_2O_3 Particles Dispersion-Strengthened Copper Base Composite, *Mater. Sci. Eng. A*, 2006, **435–436**, p 705–710
6. M.T. Marques, J.B. Correia, J.M. Criado, M.J. Diánez, and P. Matteazzi, High-temperature Stability of a Nanostructured Cu-Al_2O_3 Alloy, *Key Eng. Mater.*, 2002, **230–232**, p 652–655
7. S.H. Kim and D.N. Lee, Recrystallization of Alumina Dispersion Strengthened Copper Strips, *Mater. Sci. Eng. A*, 2001, **313**, p 24–33
8. S.H. Kim and D.N. Lee, The Effect of Rolling Conditions on the Strength and Microstructure of Dispersion Strengthened Copper Strips, *Mater. Sci. Eng. A*, 2001, **319–321**, p 471–474
9. K. Kuchařová, S.J. Zhu, and J. Čadek, Creep in Copper Dispersion Strengthened with Alumina Particles (ODS Copper), *Mater. Sci. Eng. A.*, 2003, **348**, p 170–179
10. K. Kuchařová, S.J. Zhu, and J. Čadek, Creep in ODS Copper Reinforced with Alumina Short Fibres—DRS Copper, *Mater. Sci. Eng. A*, 2003, **355**, p 267–276
11. R.K. Islamgaliev, W. Buchgraber, Y.R. Kolobov, N.M. Amirkhanov, A.V. Sergueeva, K.V. Ivanov, and G. Grabovetskaya, Deformation Behavior of Cu-Based Nanocomposite Processed by Severe Plastic Deformation, *Mater. Sci. Eng. A*, 2001, **319–321**, p 872–876
12. H. Zuhailawati and C.K. Leong, Properties and Spot Welding Behaviour of Copper-Alumina Composites Through Ball Milling and Mechanical Alloying, *Mater. Des.*, 2008, **29**(7), p 1311–1315
13. R. Thiraviam, T. Sornakumar, and A.S. Kumar, Development of Copper Alumina Metal Matrix Composite by Powder Metallurgy Method, *Int. J. Mater. Prod. Technol.*, 2008, **31**(2–4), p 305–313
14. H.K. Kang, Microstructure and Electrical Conductivity of High Volume Al_2O_3-Reinforced Copper Matrix Composites Produced by Plasma Spray, *Surf. Coat. Technol.*, 2005, **190**(2–3), p 448–452
15. G.H. Xie, S.C. Li, and W.X. Wang, Quantitatively Metallographic Analysis on the Spatial Uniformity of Particles in Particle Strengthening Metal Matrix Composite, *Phys. Test. Chem. Anal. A: Phys. Test.*, 1995, **31**(1), p 36–38 (in Chinese)
16. J. Narciso, L. Weber, and J.M. Molina, Reactivity and Thermal Behaviour of Cu–Si/SiC Composites: Effects of SiC Oxidation, *Mater. Sci. Technol.*, 2005, **22**, p 1464–1468
17. X.H. Wang, S.H. Liang, P. Yang, and Z.K. Fan, Effect of Al_2O_3 Particle Size on Vacuum Breakdown Behavior of Al_2O_3/Cu Composite, *Vacuum*, 2009, **83**, p 1475–1480